Cyclic AMP Levels, Adenylyl Cyclase Activity, and Their Stimulation by Serotonin Quantified in Intact Neurons

LELAND C. SUDLOW and RHANOR GILLETTE

From the Department of Molecular and Integrative Physiology and the Neuroscience Program, University of Illinois, Urbana-Champaign, Urbana, Illinois 61801

ABSTRACT In molluscan central neurons that express cAMP-gated Na^+ current ($I_{Na,cAMP}$), estimates of the cAMP binding affinity of the channels have suggested that effective native intracellular cAMP concentrations should be much higher than characteristic of most cells. Using neurons of the marine opisthobranch snail *Pleurobranchaea californica*, we applied theory and conventional voltage clamp techniques to use $I_{Na,cAMP}$ to report basal levels of endogenous cAMP and adenylyl cyclase, and their stimulation by serotonin. Measurements were calibrated to iontophoretic cAMP injection currents to enable expression of the data in molar terms. In 30 neurons, serotonin stimulated on average a 23-fold increase in submembrane [cAMP], effected largely by an 18-fold increase in adenylyl cyclase activity. Serotonin stimulation of adenylyl cyclase and [cAMP] was inversely proportional to cells' resting adenylyl cyclase activity. Average cAMP concentration at the membrane rose from 3.6 to 27.6 μM, levels consistent with the expected cAMP dissociation constants of the $I_{Na,cAMP}$ channels. These measures confirm the functional character of $I_{Na,cAMP}$ in the context of high levels of native cAMP. Methods similar to those employed here might be used to establish critical characters of cyclic nucleotide metabolism in the many cells of invertebrates and vertebrates that are being found to express ion currents gated by direct binding of cyclic nucleotides.

KEY WORDS: *Pleurobranchaea* • cyclic nucleotide–gated cation current • protein kinase A • H current

INTRODUCTION

Ligand-gated ion channels typically exhibit binding affinities for their ligands within the concentration range they normally encounter. For the cAMP-gated Na^+ currents ($I_{Na,cAMP}$) of molluscan neurons, maximal activation is not achieved at cAMP concentrations below 100 μM (Sudlow et al., 1993). Such high, naturally occurring concentrations of cyclic nucleotides have been inferred from conventional biochemical measurements in other cell types possessing cyclic nucleotide–gated cation currents: photoreceptor cells of retina and peripheral sensory neurons of olfactory epithelium in vertebrates (Pace et al., 1985; Stryer, 1986; Breer et al., 1990; Koutalos et al., 1995). These concentrations are many times in excess of those causing maximal activation of cAMP-dependent protein kinase (Beavo et al., 1974). In molluscan neurons, cAMP mediates both short- and long-term stimulation of excitability in both sensory neurons (Siegelbaum et al., 1982; Ocorr et al., 1985; Walsh and Byrne, 1989; Goldsmith and Abrams, 1991; Byrne et al., 1993) and neurons of motor networks (Gillette et al., 1982; Gillette and Gillette, 1983; Connor and Hockberger, 1984; Gillette and Green, 1987; Kirk et al., 1988; Kehoe, 1990; Huang and Gillette, 1991; Funte and Haydon, 1993; Price and Goldberg, 1993; Sudlow and Gillette, 1995); thus, it is of appreciable interest to know the levels of cAMP prevailing in both resting and stimulated central neurons, and the levels of synthetic activity that maintain them.

Using $I_{Na,cAMP}$ as a reporter of intracellular cAMP concentrations, we measured cAMP concentrations and adenylyl cyclase (AC)[1] activities in neurons in the locomotor network of the predatory gastropod *Pleurobranchaea californica*, where we compared the values for resting state with those obtained where AC was stimulated by the neuromodulator serotonin, 5-hydroxytryptamine (5-HT). Our results indicate that stimulated levels of cAMP are indeed in the range of tens of micromolar, and that these are achieved through correspondingly high levels of AC stimulation.

METHODS

Electrophysiology

Neurons of the "G" group of the pedal ganglia of the sea slug *P. californica* were used in all experiments. These cells are putative locomotor neurons in which $I_{Na,cAMP}$ is stimulated by 5-HT

Address correspondence to Dr. L.C. Sudlow, Department of Molecular and Integrative Physiology, University of Illinois, Urbana-Champaign, 524 Burrill Hall, 407 S. Goodwin Ave., Urbana, IL 61801. Fax: 217-333-1133; E-mail rhanor@uiuc.edu. Address reprint requests to Dr. R. Gillette, Department of Molecular and Integrative Physiology, University of Illinois, Urbana-Champaign, 524 Burrill Hall, 407 S. Goodwin Ave., Urbana, IL 61801.

[1] *Abbreviations used in this paper:* 5-HT, serotonin, 5-hydroxytryptamine; AC, adenylyl cyclase; PDE, phosphodiesterase.

J. GEN. PHYSIOL. © The Rockefeller University Press • 0022-1295/97/09/243/13 $2.00
Volume 110 September 1997 243–255
http://www.jgp.org

through activation of AC (Sudlow and Gillette, 1995). Specimens (80–500 g) of *Pleurobranchaea* were obtained from Sea Life Supply (Sand City, CA) and Pacific BioMarine (Venice, CA) and maintained in 14°C artificial sea water. Animals were anesthetized by chilling, the pedal ganglia were removed, and axotomized somata (110–240 μm diameter) were isolated and prepared for voltage clamping as previously described (Sudlow and Gillette, 1995). Artificial *Pleurobranchaea* saline consisting of (mM) 420 NaCl, 10 KCl, 25 $MgCl_2$, 25 $MgSO_4$, 10 $CaCl_2$, 10 MOPS buffered with NaOH, final pH 7.5, 14°C was constantly perfused over the cells. Cells were clamped via two-electrode voltage clamp amplifier with total cellular current reported by virtual ground amplifier. The voltage-sensing electrode was filled with 3 M KCl. A double-barreled electrode was used for current passing and cAMP iontophoresis. The current passing barrel was filled with 3 M KCl and the second barrel was filled with 200 mM cAMP (adenosine 3′:5′ cyclic monophosphate free acid; Sigma Chemical Co., St. Louis, MO), 200 mM KOH, and 20 mM Tris, pH 7.4. Resistances of both double-barreled and single pipettes were lowered by breaking back the tips against a clean capillary tube. Typical resistances for voltage and current electrodes were 4–12 and 35–80 MΩ, respectively, for the cAMP iontophoresis barrel. The double-barreled electrode was positioned at the center of the soma with a calibrated micromanipulator, as estimated from soma diameter measured with a calibrated eyepiece micrometer. All current recordings were done at a holding potential of −50 mV. Iontophoretic injections of cAMP were made with a programmable constant current source (260; WPI, New Haven, CT). Variation of iontophoretic currents over multiple injections at the same programed delivery level was negligible.

Quantification of Iontophoretic Ejections of cAMP

A transport number for cAMP iontophoresis was measured by radioimmunoassay. cAMP was iontophoresed from double-barreled electrodes (current barrel resistance 2–8 MΩ) into the mouth of a collecting siphon tube (PE 10 polyethylene tubing) flowing at 20 $\mu l \cdot min^{-1}$. Samples were collected in polypropylene microcentrifuge tubes and frozen for subsequent analysis. Saline in the reservoir from which the siphon collected was designed to mimic cytoplasmic cation composition of molluscan neurons, and contained (mM) 400 KCl, 50 NaCl, and 1 Tris, pH 7.5. Frozen samples were dried in a vacuum centrifuge (Speed-Vac; Savant Instruments, Inc., Farmingdale, NY) and radioimmunoassayed as below. cAMP delivery from three electrodes resulting from −20 and −100 nA, 50-s iontophoretic currents yielded a linear relation extrapolating to zero; an average transport number of 0.11 (0.01 SEM) was calculated from the −100 nA samples (5.79 pmol cAMP; 0.61 SEM).

Tissue Measures of cAMP

The G lobes of pedal ganglia were excised with small scissors as near-spherical clumps of cell bodies whose volumes were estimated from the approximate diameters measured by a calibrated ocular micrometer. The isolated G lobes were allowed to recover for 1 h at 14°C, and then perfused either with normal saline or saline containing 100 μM 5-HT (serotonin creatinine sulfate complex; Sigma Chemical Co.) for 5 min, after which a cold (−20°C) antifreeze solution of 1:1 (vol/vol) propylene glycol:2 M NaCl was flushed into the dish (Greenberg et al., 1987). The frozen tissue was placed in a −20°C freezer for 1–2 h, and then homogenized in a glass microhomogenizer (Radnoti Glass Technology, Inc., Monrovia, CA) in 50 μl ice-cold 65% ethanol with 10 turns of the pestle. The homogenate was transferred to a clean microcentrifuge tube and the homogenizer was washed twice with 50-μl rinses of ice-cold 65% ethanol into the microcentrifuge tube. Homogenate and rinses were mixed and immediately aliquotted for both cAMP and protein assays. Aliquots were frozen at −20°C and dried on a vacuum centrifuge. Freeze-dried aliquots were stored at −20°C until assayed. Protein concentrations were determined via the Bradford method (Bradford, 1976).

cAMP Radioimmunoassay

cAMP was measured by scintillation proximity assay (SPA), using a modified RIA protocol (Amersham Corp., Arlington Heights, IL). The SPA measures cAMP via competition between cAMP and adenosine 3′:5′-cyclic phosphoric acid 2′-*O*-succinyl-3-[^{125}I]iodotyrosine methyl ester for an antibody/scintillant microbead system. The dried samples were dissolved in 0.5 ml of 0.05 M acetate buffer immediately before assay. Samples were processed under the nonacetylation protocols for the kit. The range of sensitivity for the nonacetylation protocols of the kit was 0.2–12.8 pmol/assay tube. Aliquots (100 μl) of the samples were transferred to polypropylene scintillation vials (Sarstedt, Inc., Newton, NC). SPA analysis of the samples was performed as per package instructions and assay vials were counted on a β-scintillation counter. Data were adjusted for percent recovery, typically 90%.

5-HT Delivery

5-HT (serotonin creatinine sulfate complex; Sigma Chemical Co.) was dissolved in *Pleurobranchaea* saline and pH was adjusted to 7.5 with NaOH. A gravity-fed perfusion pipette was placed upstream of the voltage-clamped somata.

Analysis of $I_{Na,cAMP}$ Dynamics

Each soma was internally calibrated for its $I_{Na,cAMP}$ responses to iontophoretically injected cAMP. In addition to the $I_{Na,cAMP}$ amplitudes, two additional sets of measures were made during steady state injections of cAMP. First, for the pedal ganglia cells, depolarizing voltage command steps to inactivate $I_{Na,cAMP}$ were delivered from −50 (holding) to +10 mV for 100 ms. The degree of inactivation was measured as the tail current (I_{tail}) representing the net decrease in $I_{Na,cAMP}$ amplitude measured 1 s after the voltage step delivered during steady state cAMP injections or 5-HT application (Gillette and Green, 1987; Huang and Gillette, 1993; Sudlow and Gillette, 1995). The second measure examined the exponential decay rate of $I_{Na,cAMP}$ after 5-s pulsed iontophoretic injections of cAMP superimposed on the steady state injections. The data obtained during the decay were digitized and were fit by a least-squares algorithm to a time-dependent exponential decay function ($Y = X \exp(-t \cdot k_h)$) to obtain the exponential term k_h where k_h is in the units of 1/s and t is time in s. The decay rate decreased as steady state iontophoretic current delivery increased. The basal levels of $I_{Na,cAMP}$ could be calculated from either the I_{tail} or k_h values obtained during the absence of exogenous cAMP injections using the measured slope of the inactivation/$I_{Na,cAMP}$ relation, or from the slope of the $k_h/I_{Na,cAMP}$ relation.

Exponential decay slopes (k_h) of $I_{Na,cAMP}$ after 5-s pulsed injections of cAMP are directly proportional to the rate of change in [cAMP]. The decrease in [cAMP] is directly attributable to degradation by phosphodiesterase (PDE) (Huang and Gillette, 1991). While some cellular binding of cAMP may occur, buffering effects are not evident and are presumed negligible. The dose–response relationship between k_h and steady state $I_{Na,cAMP}$ responses was used to calculate a k_h for an $I_{Na,cAMP}$ response to injected cAMP of equal amplitude to the 5-HT-induced $I_{Na,cAMP}$ ($I_{5\text{-}HT}$). This equivalent k_h and the iontophoretic current equivalent for $I_{5\text{-}HT}$ were then used in Eq. 5 to calculate a cAMP concentration at the submembrane space ($[cAMP]_{memb}$). The k_h and $[cAMP]_{memb}$ obtained during 5-HT stimulation were used in Eq. 6 to calculate AC activity.

Distribution of cAMP Concentrations and AC Activity

Iontophoretic equivalents for basal and 5-HT-stimulated $I_{Na,cAMP}$ responses were calibrated on a molar basis by Eq. 1, which describes the rate of release of cAMP from an iontophoretic pipette tip (Purves, 1981):

$$q_i = In/zF \quad (1)$$

where q_i is the iontophoretic molar flux ($mol \cdot s^{-1}$), I is the iontophoretic current, n is the transport number for cAMP empirically derived for these experimental conditions, z is the valence, and F is the Faraday constant. The total amount of cAMP delivered during a steady state iontophoretic injection is equal to $q_i \cdot t$, where t is time in s.

Two additional processes are involved in the movement of cAMP out of the iontophoretic pipette: diffusional leak and bulk flow, which can both be significantly affected by the diameter of the pipette tip. Passive diffusion can be described by the relation (Purves, 1981):

$$q_d = \pi D C_{pip} \theta r_{pip} \quad (2)$$

where q_d is the diffusional leak ($mol \cdot s^{-1}$), D is the apparent diffusion coefficient ($3.3 \cdot 10^{-6}$ $cm^2 \cdot s^{-1}$) for cAMP in *Pleurobranchaea* neurons (Huang and Gillette, 1991), C_{pip} is the concentration of cAMP in the pipette (0.2 M), and θ is the included angle in radians of the pipette tip from the center axis of the pipette; typically for our pipettes the angle was 1.5°. The term r_{pip} is the inside radius (cm) of the pipette. We assumed that breakage of the double-barreled electrodes broke both barrels equally. Effective tip diameters were calculated from resistances for the current passing barrels of the double-barreled electrodes using the relation (Purves, 1981):

$$r_{pip} = (\pi \theta \sigma R_{ue})^{-1} \quad (3)$$

where σ describes the conductivity of the 3 M KCl electrolyte of the voltage clamp current barrel, nominally 0.26 $S \cdot cm^{-1}$ (Purves, 1981); and R_{ue} is the pipette resistance in ohms. Using this relationship, the range of the resistances of the current passing electrodes corresponded to tip diameters of 0.08–0.23 μm.

Bulk flow arises from hydrostatic pressure effects imposed at the pipette tip by gravity by the relation (Purves, 1981):

$$q_h = 3\pi \theta p g h C_{pip} r_{pip}^{\ 3} (8\eta)^{-1} \quad (4)$$

where q_h is the hydrostatic bulk flow ($mol \cdot s^{-1}$), p is the viscosity (1,000 $kg \cdot m^{-3}$), g is gravitational attraction (9.8 $m \cdot s^{-2}$), h is the height of cAMP solution in the iontophoretic barrel (m), and η is the viscosity of the cAMP solution (0.001 Pa·s). The terms θ, C_{pip}, and r_{pip} have the same meanings as above. Diffusional leak and hydrostatic bulk flow of cAMP from the cAMP iontophoresis barrels were calculated to have contributed to <3 $fmol \cdot s^{-1}$ cAMP under these conditions given the pipette diameters involved (Krnjević et al., 1963; Purves, 1981). In radioimmunoassays of sample aliquots taken after 300 s of diffusion with low resistance iontophoretic electrodes, cAMP levels did not register above the kit's detection limits (0.2 pmol/aliquot).

The steady state distribution of a solute (such as cAMP) released from a point source (the injection electrode) in a finite spherical space with an impermeable boundary (the axotomized neuron soma), in which a first-order decay occurs, is described by Eq. 5 (Purves, 1976, 1977):

$$C(r) = \frac{q_i}{4\pi r D} \frac{(r_n\sqrt{k_h/D}+1)\, e^{r\sqrt{k_h/D}} + (r_n\sqrt{k_h/D}-1)\, e^{(2r_n - r)\sqrt{k_h/D}}}{(r_n\sqrt{k_h/D}+1) + (r_n\sqrt{k_h/D}-1)\, e^{2r_n\sqrt{k_h/D}}} \quad (5)$$

where $C(r)$ is cAMP concentration at radius r, q_i is the iontophoretic injection flux described by Eq. 1, r_n is the radius of the cell membrane, k_h is the relaxation rate constant for $I_{Na,cAMP}$ elicited by I in Eq. 1, and D has the same value as above. We assumed the simplest cases where PDE activity is distributed homogeneously in the cytoplasm and there are no significant internal diffusion barriers (see Huang and Gillette, 1991). The exponentially decreasing gradient from pipette tip to cell membrane described by Eq. 5 is largely influenced by the diameter of the neuron and PDE, which is reflected in k_h. Eq. 5 was simplified from its original form since the radius of the release point has no significant impact on the computations as long as the inside diameter of the pipette is <4 μm. In practice, our pipette tip diameters were <1 μm.

RESULTS

5-HT Depolarizes Neurons via $I_{Na,cAMP}$

We related quantitative cAMP injections to steady state $I_{Na,cAMP}$, its inactivation characteristics, exponential decay rates, and measurements of current saturation. $I_{Na,cAMP}$ reaches a steady state condition during tonic iontophoretic cAMP injections (Fig. 1). At nonsaturating levels, the amplitude of elicited $I_{Na,cAMP}$ increases linearly with the iontophoretic current (Figs. 1 and 2 *A*). Although most experiments were performed in the nonsaturating range of the iontophoretic current/$I_{Na,cAMP}$ dose–response function, some experiments were designed to specifically examine the saturability of $I_{Na,cAMP}$ by iontophoretic current. The $I_{Na,cAMP}$ responses did saturate at high current (>−200 nA) iontophoretic injections of cAMP (Fig. 3). These iontophoretic current/$I_{Na,cAMP}$ saturation measures were not typically performed in most experiments, due to adverse long term consequences on the viability of the cell and on diminishing amplitude and lengthening duration of $I_{Na,cAMP}$ after prolonged saturating injections of cAMP.

$I_{Na,cAMP}$ in pedal neurons is inactivated by Ca^{2+} influx caused by depolarizing voltage steps (Fig. 1); after such a step, inactivation is manifested as a slowly decaying tail current (I_{tail}; Gillette and Green, 1987; Huang and Gillette, 1993). When brief depolarizing voltage steps are delivered to otherwise unstimulated cells, small tail currents are observed resulting from inactivation of basal $I_{Na,cAMP}$. The I_{tail} amplitude increases linearly with the inward current induced during either tonic iontophoretic injections of cAMP or bath application of 5-HT, indicating the origin in $I_{Na,cAMP}$ (Figs. 1 and 2 *B*).

Exponential decay slopes (k_h) of $I_{Na,cAMP}$ after 5-s pulse injections of cAMP were also dependent on the steady state level of $I_{Na,cAMP}$ in the cell (Fig. 1), with k_h decreasing with increasing injections of cAMP (Fig. 2 *C*). This relationship between k_h and steady state $I_{Na,cAMP}$ was linear when the iontophoretic injections were below saturation levels for $I_{Na,cAMP}$. The relaxation rate k_h is highly sensitive to PDE inhibitors (Aldenhoff et al., 1983; Connor and Hockberger, 1984; Huang and Gillette,

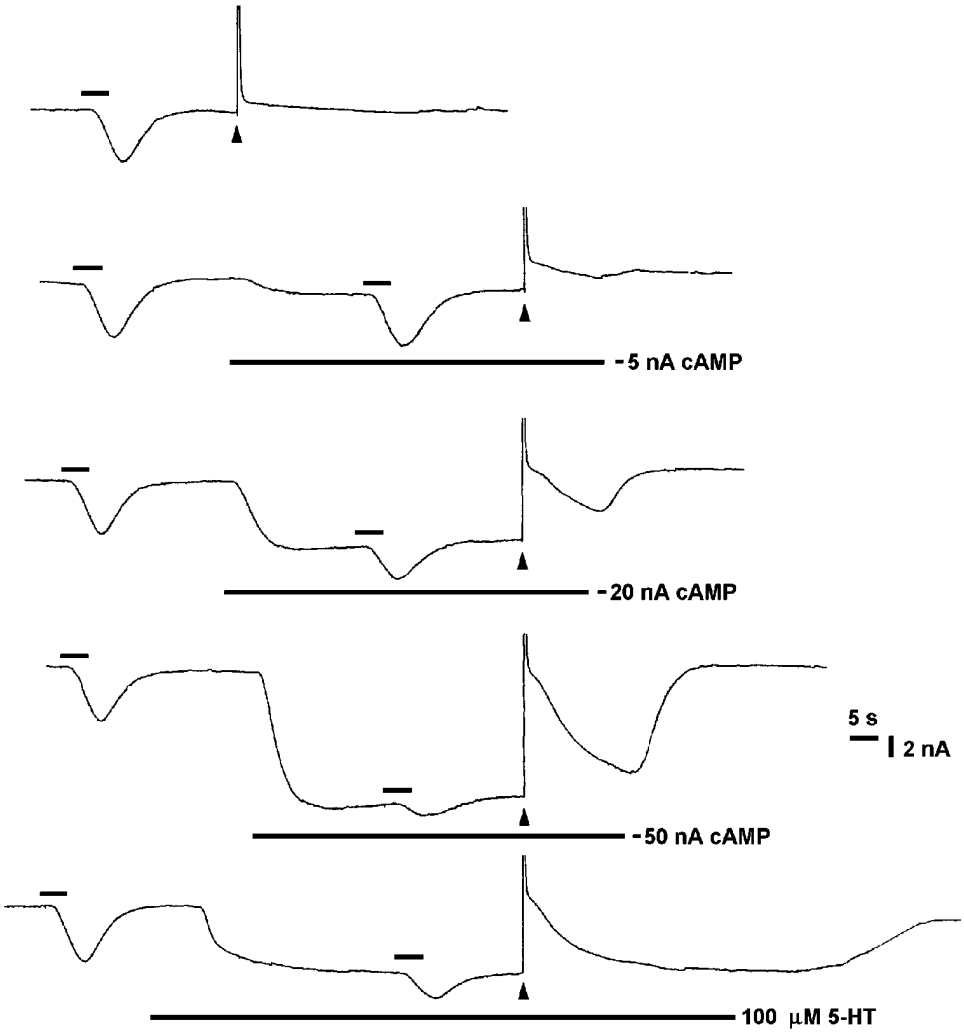

FIGURE 1. Dose–response relation for iontophoretically injected cAMP vs. characteristics of the $I_{Na,cAMP}$ response. Test pulse injections (*short bars*, 5 s, −10 nA) were delivered before and during tonic iontophoretic injections of cAMP and during bath application of 5-HT. The steady state $I_{Na,cAMP}$ response, the exponential decay rate (k_h) after the 5-s test pulse injections, and degree of occlusion were obtained from these records. Depolarizing voltage steps (*arrows*, from −50 to +10 mV, 100 ms) were also delivered before and during tonic iontophoretic injections of cAMP to measure amplitudes of the slowly decaying tail currents. The level of inactivation was arbitrarily taken as the decrease of $I_{Na,cAMP}$ measured 1 s after the voltage step. The tail current amplitude is a function of the summed inactivation of basal and induced $I_{Na,cAMP}$ (Huang and Gillette, 1991; Sudlow and Gillette, 1995). Leakage current for this soma was −1.5 nA.

1991) and is a quantitative index of PDE-mediated degradation of cAMP (Huang and Gillette, 1991). PDE inhibitors, such as 3-isobutylmethylxanthine, cause dose–dependent decreases in the decay rate k_h and increases in the cAMP levels in the soma without change in adenylyl cyclase activities (Sudlow and Gillette, manuscript in preparation).

The steady inward current stimulated by 5-HT ($I_{5\text{-}HT}$) occludes the $I_{Na,cAMP}$ response to iontophoretic pulsed injections of cAMP (Figs. 1 and 2 *D*). $I_{5\text{-}HT}$ in the pedal neurons is largely composed of $I_{Na,cAMP}$, whose levels can be calculated from inactivation (Sudlow and Gillette, 1995) or measures of k_h saturation (see further). The degree of occlusion was also indicative of the degree of saturation of $I_{Na,cAMP}$ by iontophoretic current. As the iontophoretically elicited $I_{Na,cAMP}$ approached saturation, the degree of occlusion also increased.

$I_{Na,cAMP}$ Responses Report on AC Stimulation and [cAMP]

Since $I_{Na,cAMP}$ is a direct function of the cAMP concentration, the amplitude of the current is the balanced result of the activities of the synthetic and degradative enzymes, AC and PDE, respectively (Huang and Gillette, 1991; also see Hodgkin and Nunn, 1988). Knowledge of the cAMP concentration and of the activity of at least one of the enzymes would allow the calculation of the remaining enzyme's activity at steady state. However, in the living cell, unlike the biochemist's reaction vessel, such a calculation must take into account the compartmentalization and geometry of the cell and the kinetics of cAMP diffusion and degradation. In the neuron, AC is bound at the plasma membrane, while PDE is distributed in the cytoplasm in both soluble and membrane-bound fractions (Fell, 1980; Shakur et al., 1993; Bolger, 1994). Thus, we took into account the existence of a gradient of cAMP concentrations. During neurotransmitter stimulation of the soma, this cAMP concentration gradient is highest next to the membrane and falls exponentially with distance towards the center of the cell (Fell, 1980; Bacskai et al., 1993; Shakur et al., 1993; Bolger, 1994).

AC activity was calculated from the $I_{Na,cAMP}$ records obtained before and during bath applications of 5-HT.

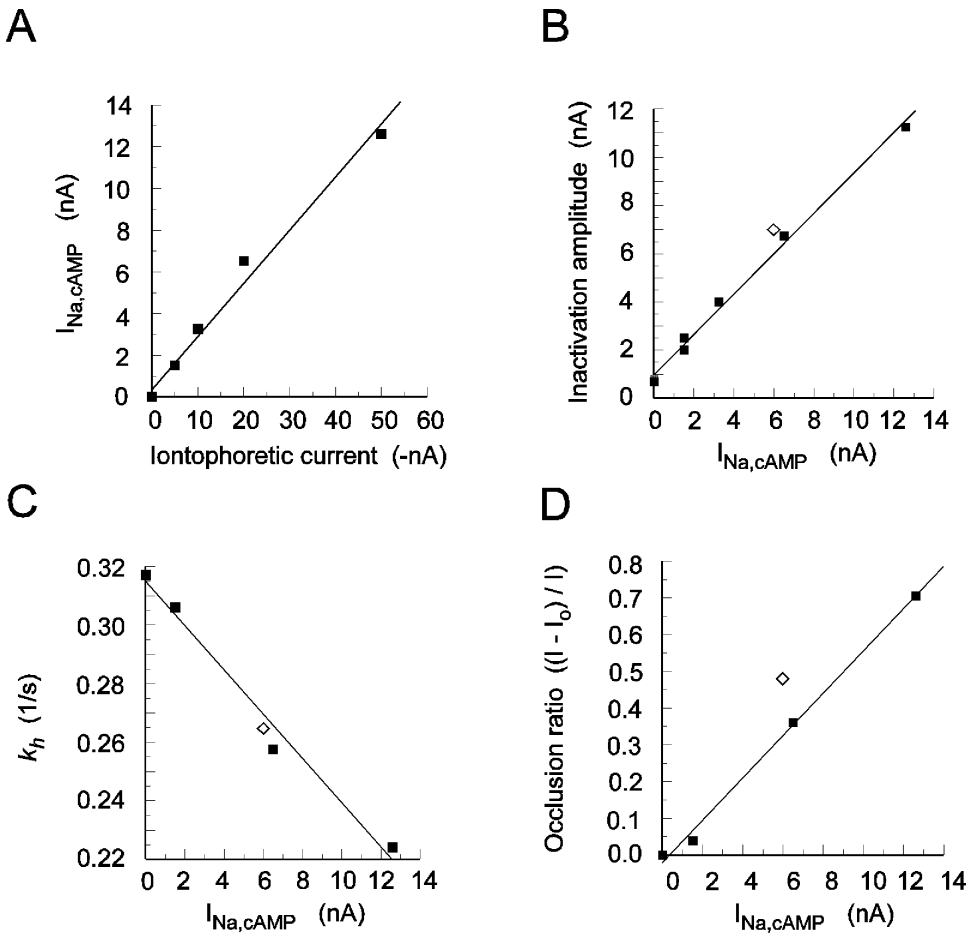

FIGURE 2. Relationships between iontophoretic current and $I_{Na,cAMP}$, and among $I_{Na,cAMP}$ and inactivation, k_h and occlusion for the data of Fig. 1. (*A*) The dose–response relation for cAMP injection current and steady state $I_{Na,cAMP}$ response was linear at low injection currents. (*B*) Inactivation tail current amplitudes were plotted against steady state $I_{Na,cAMP}$ induced by iontophoretic cAMP injection (■) or $I_{5\text{-}HT}$ during bath addition of 10 μM 5-HT (◇). The linear slope of the relation represents the fractional inactivation of $I_{Na,cAMP}$ by the depolarizing pulse and thus permits calculation of basal $I_{Na,cAMP}$ in the absence of exogenous cAMP injection (Huang and Gillette, 1991; Sudlow and Gillette, 1995) and during 5-HT stimulation. The $I_{Na,cAMP}$ equivalent for the inactivation measured during 5-HT treatment was 7.2 nA, corresponding to a 26.9 nA iontophoretic injection equivalent. (*C*) Exponential decay slopes (k_h) were plotted against steady state $I_{Na,cAMP}$ elicited by tonic iontophoretic injection (■) or by application of 5-HT (◇). The linear slope of the relation represents the proportional slowing of the k_h associated with higher levels of $I_{Na,cAMP}$ and can allow the determination of basal $I_{Na,cAMP}$. (*D*) Occlusion of $I_{Na,cAMP}$ test pulse responses were measured against steady state $I_{Na,cAMP}$ induced by tonic cAMP injection (see Fig. 1). Occlusion ratios were obtained from the relation $(I - I_o)/I$ (Huang and Gillette, 1993; Sudlow and Gillette, 1995), where I is the amplitude of $I_{Na,cAMP}$ elicited by a 5-s pulse of cAMP delivered in the absence of steady state $I_{Na,cAMP}$ induced by cAMP injection or by 5-HT. I_o is the amplitude of $I_{Na,cAMP}$ elicited by pulse injection of cAMP superimposed during tonic injections of cAMP or bath application of 5-HT. Most somata exhibited occlusion ratios during $I_{5\text{-}HT}$ similar to $I_{Na,cAMP}$ of equal amplitude evoked by iontophoretic injection of cAMP. The lines are the best fits from least-squares analysis of the data.

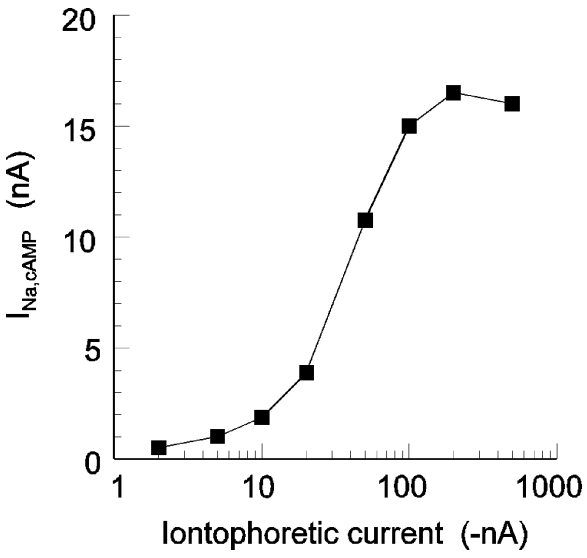

The responses of the cell were calibrated using three relationships based upon direct experimental measures: (*a*) the dose–response relation of tonic cAMP iontophoretic current to the induced steady state $I_{Na,cAMP}$ (see Fig. 2 *A*); (*b*) the dose–response relation of steady state $I_{Na,cAMP}$ current amplitudes to depolarization-induced inactivation (see Fig. 2 *B*), which allowed estimation of $I_{Na,cAMP}$ in the absence of cAMP injection; and (*c*) the dose–response relation of the steady state $I_{Na,cAMP}$ to k_h

FIGURE 3. Saturability of the iontophoretic current/steady state $I_{Na,cAMP}$ relation. Voltage clamped somata ($n = 4$) were injected with iontophoretic currents ranging from −2 to −500 nA (90–180 s) and steady state $I_{Na,cAMP}$ response characteristics were determined. For this representative cell, steady state $I_{Na,cAMP}$ increased in a dose-dependent manner up to the −100 nA injections, above which $I_{Na,cAMP}$ exhibited saturation.

(see Fig. 2 *C*) obtained during steady state $I_{Na,cAMP}$, which also allowed for the estimation of basal $I_{Na,cAMP}$ (Huang and Gillette, 1991). Resting and 5-HT-stimulated levels of $I_{Na,cAMP}$ were calculated using the resting and 5-HT-stimulated inactivation measures and the linear regression coefficients of the inactivation/steady state $I_{Na,cAMP}$ relation (see Fig. 2 *B*). The k_h values associated with the steady state $I_{Na,cAMP}$ equivalents for resting and 5-HT-stimulated states were determined from the $I_{Na,cAMP}$ equivalents and the linear regression coefficients of the k_h/steady state $I_{Na,cAMP}$ dose–response relation (see Fig. 2 *C*). The steady state $I_{Na,cAMP}$ equivalents were translated into iontophoretic cAMP injection equivalents using the linear regression coefficients of the dose–response relation of tonic injection current to induced $I_{Na,cAMP}$ (see Fig. 2 *A*). These iontophoretic equivalents, along with their equivalent k_h values, were adjusted for diffusion and hydrolysis by Eq. 5 to estimate $[cAMP]_{memb}$. Last, AC activities were calculated from the $[cAMP]_{memb}$ and the k_h during 5-HT-stimulated state using Eq. 6. We derived Eq. 6 (APPENDIX) to explicitly describe the active synthesis, degradation, and inward diffusion of an enzymatic product from the boundary of an impermeable sphere:

$$C(r) = \frac{Q_{AC}}{4\pi r D} \frac{\sinh\left(r\sqrt{k_h/D}\right)}{\left(r_n\sqrt{k_h/D}\right)\cosh\left(r_n\sqrt{k_h/D}\right) - \sinh\left(r_n\sqrt{k_h/D}\right)} \quad (6)$$

where $C(r)$ is [cAMP] at radius r, taken here as the compartment 100 nm subjacent to the cell membrane. Q_{AC} is the flux of the membrane-bound AC expressed in terms of $mol \cdot s^{-1}$. The variables r, r_n, k_h, and D have the same meanings as in Eq. 5. The equation was derived with the assumption that PDE is homogeneously distributed in the soma. After calculating $[cAMP]_{memb}$ with Eq. 5, Eq. 6 is solved for Q_{AC}. With the soma diameter, AC activity is normalized to the surface area of the soma ($mol \cdot s^{-1} \cdot cm^{-2}$) to allow ready comparison of different cells.

The results of measurements on 30 neurons are summarized in Table I. In unstimulated cells, the distribution of basal $[cAMP]_{memb}$ was markedly skewed to lower values with a few rare higher values (Fig. 4); AC activities were distributed similarly. Stimulation of AC by 5-HT shifted the distribution of responses towards markedly higher values (Fig. 4). The non-Gaussian distributions of $[cAMP]_{memb}$ and AC activities contributed to wide variation among the calculated means and standard deviations. When cAMP concentrations and AC activities in bilaterally homologous neurons from the pedal ganglia of the same animal were examined (see Table I, cells A and B, E and F, and K and L), the levels were very comparable. However, when cAMP concentrations and AC activities in different, nonhomologous neurons of the same animal were compared (see Table I, cells F vs. G, I vs. J, and P vs. Q), levels varied substantially. Thus, variability of the cAMP and AC measures is likely to arise from phenotypic variation in the cell population under study. 5-HT stimulation augmented $[cAMP]_{memb}$ from 1.16- to 82.60-fold, averaging 23.35- ± 21.96-fold (μM ± SD), and AC from 1.17- to 89.68-fold, with an average stimulation of 18.56- ± 18.79-fold. The average resting $[cAMP]_{memb}$ was 3.64 ± 8.59 (μM ± SD). Adjusting for the PDE-induced gradient in cell bodies yields an integrated average whole-cell concentration of 2.54 ± 2.61 μM. 5-HT stimulation raised $[cAMP]_{memb}$ to 27.68 ± 30.12 μM and whole-cell integrated [cAMP] to 20.60 ± 23.61 μM. Similarly, resting AC activities averaged $2.44 \pm 5.26 \times 10^{-12}$ $mol \cdot s^{-1} \cdot cm^{-2}$ and were elevated by 5-HT stimulation to $15.96 \pm 16.21 \times 10^{-12}$ $mol \cdot s^{-1} \cdot cm^{-2}$. When these AC activities are expressed in terms of cell volume, as $\mu M \cdot s^{-1}$ (micromol·liter^{-1}·s^{-1}), basal AC was 0.83 ± 1.64 $\mu M \cdot s^{-1}$ and stimulated AC rates (basal + 5-HT stimulated) were 5.55 ± 6.92 $\mu M \cdot s^{-1}$.

Tissue Measures of [cAMP]

Radioimmunoassays of basal levels of cAMP in the G lobes yielded an average value of $0.82 \pm 0.45 \times 10^{-12}$ $mol \cdot (\mu g\ protein)^{-1}$ (μM ± SD; $n = 2$). We used a presumedly maximal stimulatory concentration of 5-HT (100 μM; see Fig. 7) to observe the upper end of cAMP production. Such stimulation elevated cAMP to $9.08 \pm 1.95 \times 10^{-12}$ $mol \cdot (\mu g\ protein)^{-1}$ ($n = 5$) within a range of $6.38–11.46 \times 10^{-12}$ $mol \cdot (\mu g\ protein)^{-1}$. The protein concentration per unit volume, measured by Bradford assay, was 8.5 $\mu g \cdot \mu l^{-1}$. With this conversion factor, the electrophysiological measures of whole cell [cAMP] (Table I) could be directly compared with the radioimmunoassays. The radioimmunoassayed levels of unstimulated G lobes were 6.97 ± 3.84 μM and levels during stimulation with 100 μM 5-HT were 77.15 ± 16.86 μM within a range of 54.2–97.38 μM. This compares with the electrophysiological measures of [cAMP] in unstimulated somata of 3.64 ± 8.59 μM ($n = 30$), within a range of 0.08–28.88 μM, and 10 μM 5-HT-stimulated whole cell [cAMP] of 20.60 ± 23.61 μM, within a range of 1.73–96.90 μM. Results of both biochemical and electrophysiological assays agree that 5-HT stimulates high levels of cAMP.

$I_{Na,cAMP}$ Binding Affinity

We next examined the apparent binding affinity of cAMP in activating $I_{Na,cAMP}$. The apparent binding affinity for cAMP is an inverse function of intracellular $[Ca^{2+}]$ in the G cells (Huang and Gillette, 1993), and is a minimum estimate of actual binding affinity. The $I_{Na,cAMP}$ elicited for each tonic iontophoretic injection and the $[cAMP]_{memb}$ determined for that injection were

TABLE I

Basal and 5-HT-stimulated [cAMP] and AC Activities in Single Cells

	Basal			5-HT	Total (Basal + 5-HT stimulation)			
							Activation ratio	
Cell	$I_{Na,cAMP}$	$[cAMP]_{memb}$	AC (Q_{Basal})	Response $I_{5\text{-}HT}$	$[cAMP]_{memb}$	AC (Q_{Total})	$[cAMP]_{Total}$:$[cAMP]_{Basal}$	Q_{total}:Q_{Basal}
	$-nA$	μM	$picomol \cdot s^{-1} \cdot cm^{-2}$	$-nA$	μM	$picomol \cdot s^{-1} \cdot cm^{-2}$		
A	0.91	1.29	1.25	1.00	2.97	2.72	2.30	2.18
B	1.45	1.91	2.29	1.00	3.23	3.88	1.69	1.69
C	2.88	0.69	0.80	10.25	4.67	4.98	6.77	6.22
D	0.32	0.13	0.11	5.25	5.59	4.10	44.07	35.76
E	0.72	0.35	0.30	6.50	11.59	8.71	33.11	28.62
F	0.35	0.31	0.29	6.25	13.62	11.32	44.21	38.37
G	0.23	1.06	0.72	8.50	57.61	34.99	54.24	48.80
H	1.16	5.28	3.80	8.50	53.13	37.58	10.07	9.89
I	0.97	0.96	0.78	8.50	31.66	16.41	33.01	21.01
J	1.81	2.09	1.78	2.00	4.13	3.17	1.97	1.78
K	0.84	1.41	0.97	3.00	11.23	6.80	7.95	7.04
L	1.01	1.40	0.99	6.00	12.02	8.16	8.56	8.25
M	0.10	0.36	0.24	1.45	9.16	5.79	25.17	24.44
N	1.70	0.28	0.23	4.75	3.42	3.02	12.21	13.13
O	1.75	7.10	5.15	2.50	13.91	11.06	1.96	2.15
P	0.87	0.95	0.59	3.25	4.78	3.07	5.01	5.23
Q	0.21	0.41	0.29	5.50	33.78	25.92	82.60	89.68
R	0.60	5.05	4.50	6.50	99.22	59.93	19.66	13.33
S	1.75	2.99	3.02	7.38	60.59	58.65	20.28	19.45
T	0.99	21.26	10.86	1.35	48.85	21.55	2.30	1.98
U	0.10	0.31	0.35	3.75	9.36	8.14	30.25	23.38
V	4.92	43.71	27.89	1.50	50.65	32.62	1.16	1.17
W	0.81	2.26	1.46	10.75	31.46	15.62	13.91	10.68
X	0.26	0.29	0.26	5.75	9.61	7.93	32.85	30.50
Y	0.16	1.07	0.70	7.50	66.56	24.91	62.21	35.59
Z	0.15	0.58	0.40	4.50	40.35	11.79	69.57	29.46
AA	0.32	0.71	0.60	2.80	5.50	3.60	7.75	6.01
BB	0.27	0.16	0.18	5.00	3.49	2.80	21.81	15.56
CC	0.59	0.72	0.55	6.50	9.04	2.30	12.55	4.18
DD	2.33	3.83	1.73	3.00	119.35	37.23	31.16	21.52
Mean		3.64	2.44		27.68*	15.96*	23.35	18.56
SD		8.59	5.26		30.12	16.21	21.96	18.79

*Significantly different from control levels; $P < 0.0001$, Mann-Whitney U test.

fit by least-squares analysis to the modified Hill equation (Huang and Gillette, 1991):

$$I = I_{max}[cAMP]_{memb}/([cAMP]_{memb} + K_c) \quad (7)$$

where I_{max} is the maximum available $I_{Na,cAMP}$ and K_c is the apparent cAMP dissociation constant for the $I_{Na,cAMP}$ channels. The average I_{max} was 20.92 ± 16.53 nA (n = 17) within a range of 6.84–90.62 nA. The average K_c for the $I_{Na,cAMP}$ current was 18.05 ± 8.95 μM (n = 17) within a range of 4.32–34.05 μM. For experiments designed to examine the interaction between 5-HT and $I_{Na,cAMP}$, the calculated $[cAMP]_{memb}$ and nonsaturating $I_{Na,cAMP}$ levels were fit by a least-squares algorithm of Eq. 7. Additional experiments were designed to specifically examine the entire dose–response relation between iontophoretic current and $I_{Na,cAMP}$ (see Fig. 3). The relation, presented in terms of the $[cAMP]_{memb}/I_{Na,cAMP}$ response, was fitted well by Eq. 7 (Fig. 5). The I_{max} and K_c for the data in Fig. 3, calculated as per above, were 16.86 nA and 22.12 μM, respectively. These values are consistent with cAMP dissociation constants for $I_{Na,cAMP}$ channels thought to be at least several tens of micromolar or greater (Aldenhoff et al., 1983; Green and Gillette, 1983; Connor and Hockberger, 1984; Sudlow et al., 1993).

The net increase in AC activation stimulated by 5-HT was inversely proportional to resting AC rates (Fig. 6). In general, cells that exhibited comparatively high basal

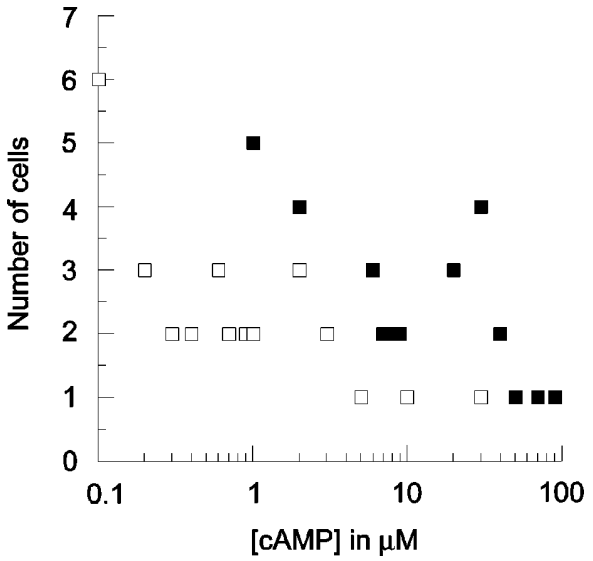

FIGURE 4. Frequency distribution histogram of whole cell cAMP concentrations in unstimulated (□) and 5-HT-stimulated (■) somata. Bins were set 0.1-μM wide for the range 0–1 μM, 1-μM for 1–10 μM, and 10 μM for 10–100 μM.

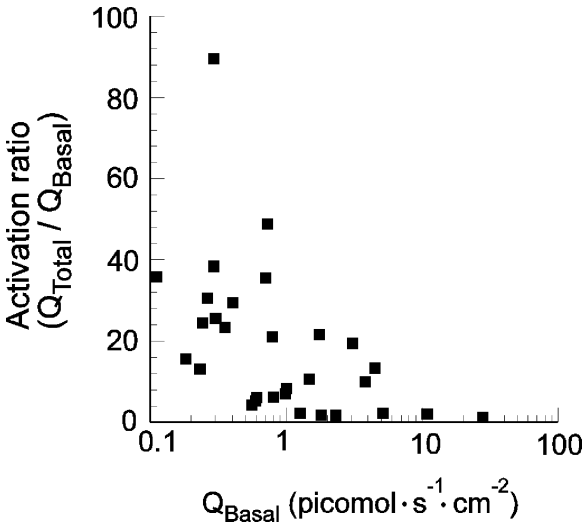

FIGURE 6. Cells with lower basal AC rates showed greater stimulation by 5-HT than those with higher rates. The histogram shows the relationship of AC activation to basal (unstimulated) rates. Activation ratios for 5-HT-stimulated AC activity were compared with their prestimulation basal AC activity.

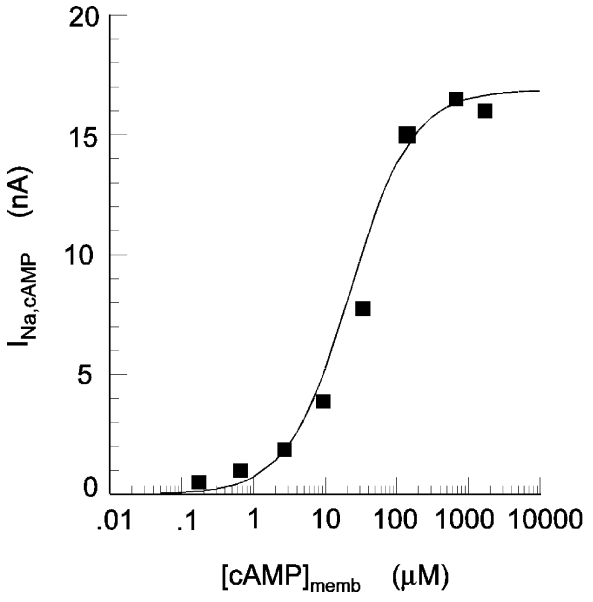

FIGURE 5. Saturability of $I_{Na,cAMP}$ by increasing levels of $[cAMP]_{memb}$. Measures of $I_{Na,cAMP}$, inactivation, and k_h were obtained during tonic injections ranging from −2 to −500 nA. The results were used in Eq. 5 to calculate $[cAMP]_{memb}$. The $I_{Na,cAMP}$ response and the calculated $[cAMP]_{memb}$ were used in Eq. 7 via a least-squares algorithm to examine the I_{max} (maximum $I_{Na,cAMP}$ available) and K_c (the apparent dissociation constant of the channels for cAMP, in micromolar). The filled squares represent the experimental $I_{Na,cAMP}$ and the calculated $[cAMP]_{memb}$. The line represents the least-squares analysis best fit of Eq. 7.

AC rates (see Table I) showed appreciably less stimulation by 5-HT than cells with low basal activity. Collectively, these data indicate that cyclase activity varies in its basal levels of activation among different cells and preparations, perhaps due to effects of dissection, endogenous neuromodulators, or other unknown factors.

5-HT elicited similar concentration-dependent effects in pairs of bilaterally homologous neurons (Fig. 7). Measured values of AC activation with increasing 5-HT concentrations for bilateral homologs (Table I, cells K and L) were similar, reaching a plateau phase above 10 μM 5-HT (Fig. 7).

DISCUSSION

The present findings document high average resting levels of submembrane cAMP in unstimulated neurons, in excess of 3.64 μM, within a wide range of 0.13–44 μM. The whole cell levels of cAMP were 2.54 μM within a range of 0.07–50 μM, which corresponded well with the radioimmunoassay measures of cAMP in *Pleurobranchaea* G lobes homogenates of 6.97 μM. These values are also similar to the results of radioimmunoassays of homogenates of large peripheral effector neurons of *Aplysia*, neurons similar in function to those studied here, that yielded resting levels of cAMP of 1–6 μM (Hockberger and Yamane, 1987). These values in *Pleurobranchaea*, even at the lower limit, are considerably higher than the resting levels of <50 nM in the somata of cultured *Aplysia* sensory neurons, as estimated from cAMP binding-induced fluorescence changes in fluoro-

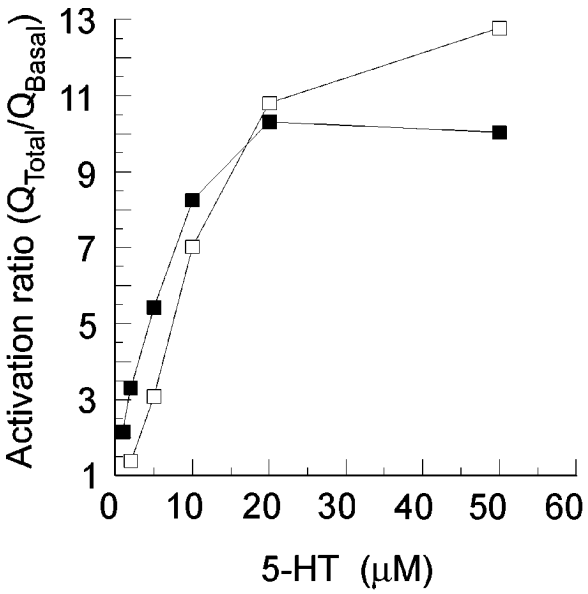

FIGURE 7. 5-HT dose-dependent increase in AC activities. The dose–response relationship was compared in a pair of bilaterally homologous G cell neurons from a single animal, identifiable by position and size. 5-HT concentration-dependent increases in AC activation ratios reached plateaus above 10 μM 5-HT.

phore-labeled subunits of PKA (Bacskai et al., 1993). This is unlikely to result from a species difference between *Aplysia* and *Pleurobranchaea*, since our unpublished observations on identified effector neurons of *Aplysia* (R2 and L10 of the abdominal ganglion) exhibiting $I_{Na,cAMP}$ show that they require a similar range of iontophoretic current to activate the current. The differences in values for [cAMP] between sensory and effector neurons may well be adaptively related to the expression of $I_{Na,cAMP}$ in the effector neurons. $I_{Na,cAMP}$ is probably not significant in the sensory neurons; they are well studied and a prominent $I_{Na,cAMP}$ would doubtless have been reported previously. Thus, these results suggest that cAMP levels tend to be higher in neurons that express $I_{Na,cAMP}$ than in those that lack it. This interpretation is consistent with observations on vertebrate retina and olfactory tissues, where cyclic nucleotide levels in cells expressing similar cGMP- or cAMP-gated cation currents attain similarly high values.

In 5-HT-stimulated somata the average whole cell cAMP levels rose to nearly 21 μM. Because of the concentration gradient for cAMP caused by asymmetric distribution of AC and PDE, the actual average submembrane values exceeded 27 μM and in several cases approached 100 μM (Table I). Observations on single $I_{Na,cAMP}$ channels in excised patches showed that the probable cAMP dissociation constant was probably in excess of some tens of micromolar (Sudlow et al., 1993), a conclusion in accord with observations on the macro-current (Aldenhoff et al., 1983; Green and Gillette, 1983; Connor and Hockberger, 1984; Sudlow et al., 1993). In the present measures, we found that the average dissociation constant for cAMP binding in activation of $I_{Na,cAMP}$ was about 18 μM, within a range of 4.32–34.05 μM. The wide variation in the apparent binding affinity for cAMP is likely to arise in large part from the fact that it is a function of intracellular $[Ca^{2+}]$ in the G cells, which acts like a competitive inhibitor of cAMP binding to the channel (Huang and Gillette, 1993); other modes of channel regulation, such as phosphorylation (see Wilson and Kaczmarek, 1993), are also possible. The present observations support the expectation for the relatively low binding affinity for cAMP in activation of the macro-$I_{Na,cAMP}$ in the intact neuron. They also show that the high endogenous levels of cAMP needed to activate the current are actually attained during stimulation with the natural neuromodulator.

The system of equations presented in this study incorporates an assumption of homogeneous distribution of PDE in the soma. This assumption stems from observations of Huang and Gillette (1991), who varied the depth of the iontophoretic pipette and examined the exponential decay rates of $I_{Na,cAMP}$ after pulse injections of cAMP; they found no variation of k_h with depth. If PDE were significantly excluded from the nuclear core of the soma, and PDE were concentrated in the rind of the cytoplasm much like the distribution of regulatory subunit of PKA observed by Bacskai et al. (1993), then the exponential decay after a pulse injection of cAMP should have slowed as the pipette penetrated further to the center of the cell, where the PDE-free zone would have acted as a cAMP reservoir. Instead, the modeling of the time course of the response of $I_{Na,cAMP}$ to a pulse injection was best fit by a homogenous distribution of PDE, where depth and PDE activity accounted for the response's characteristics and time course (Huang and Gillette, 1991). We are not aware of direct immunocytochemical documentation for the distribution of molluscan PDE in the soma. If in the future it should be found that *Pleurobranchaea* G neurons have substantial regions of the soma devoid of PDE, the results presented in this report will be underestimations of the cAMP levels of the cells in Table I. Conversely, a second nonhomogenous distribution of PDE could involve a thin region of high PDE activity subjacent to the neurolemma. Careful examination of the performance of the equations indicated that as long as the region of high PDE activity (i.e., $2 \cdot k_h$) involved $<14\%$ of the total volume of the cell, the consequences to the cAMP calculations amounted to $<1\%$ variations in the results. The equations function not only due to the effects of k_h and diffusion, but through the distance that the cAMP has to diffuse. If the region of high PDE activity is only a few mi-

crons thick near the neurolemma, the consequences to the computations are negligible.

The [cAMP] and AC activities presented in Table I exhibit fairly large variation reflected in the means and standard deviations calculated for the sample. Some of the variability during resting measures can be accounted for by the extremely high levels of cAMP and AC in the two cells T and V, which appeared to be maximally activated in the basal state. The high levels associated with those cells are indicative of significant AC activation at the time of the experimental measures. During 5-HT stimulation, the measures associated with cells R and DD contributed to the variance of cAMP and AC measures. The levels of cAMP associated with cells R and DD, while high, are similar to the radioimmunoassay measures of cAMP obtained during 5-HT treatment, and thus appear to be within physiological range. It is highly unlikely that errors in the measures of k_h would account for the large sums of squares associated with the measures in Table I. We examined the performance of the equations and found that for a given model cell, iontophoretic current, and k_h, k_h would have to be underestimated by >60% to reach cAMP values in excess of the mean $[cAMP]_{memb}$, 27.6 μM. Typically, <2% variability was observed in repeated exponential slope measurements of k_h of the same $I_{Na,cAMP}$ response to cAMP pulse injection. The production of cAMP during 5-HT treatment falls into two major categories, cells that respond with cAMP levels between 2.97 and 13.91 μM with a mean and standard deviation of 7.63 ± 3.82 μM (n = 18) and those cells that respond with cAMP production between 31.46 and 119.35 μM with a mean and standard deviation of 57.97 ± 26.92 μM (n = 12) ($P < 0.0001$, Mann-Whitney U test). It appears that different *Pleurobranchaea* G neurons vary greatly in cAMP production in response to 5-HT and it is this phenotypic variation that accounts for the variability of the individual cell measures. This was borne out by the observations on nonhomologous neurons from pedal ganglia of the same animal (Table I: cells F vs. G, I vs. J, and P vs. Q).

The radioimmunoassay measures of cAMP of whole *Pleurobranchaea* G lobe homogenates were higher than most of the cellular measures of Table I. These homogenates involved not only somata, but neuropil as well. cAMP levels in dendrites have been shown to be significantly higher than that observed in the somata in *Aplysia* sensory neurons (Bacskai et al., 1993). The higher levels of cAMP measured in the RIA as compared with the cellular measures may reflect, in part, the contributions of a higher neuropilar stimulation of cAMP production by 5-HT. Additionally, the neurons of the G lobes of the animals used in the RIA as a group may have been prone to produce cAMP at higher levels, like that observed in Table I, cells R, Y, and DD.

The average 18-fold stimulation of AC activity, and the increases shown by some neurons up to nearly 90-fold, are appreciably higher than values reported for in vitro measures of molluscan nervous tissue, which may vary from 0.75- to 7-fold in homogenates of *Aplysia* sensory neurons (Yovell et al., 1987; Eliot et al., 1989; Abrams et al., 1991; Goldsmith and Abrams, 1991; Yovell and Abrams, 1992). These differences could result from variation in AC activity among cells on the basis of whether or not they express $I_{Na,cAMP}$. Alternatively, or in addition, the considerable differences between in vitro and in vivo stimulation may well arise from the disruption of the intracellular environment inherent to in vitro assays. In particular, homogenization may greatly reduce the capacity for AC activity by dilution of the G protein cofactors and disruption of the tubulin that interacts with the G proteins. This interpretation is suggested from observations on adrenergic stimulation of AC in an assay system where cells are detergent permeabilized, but remain otherwise intact; AC stimulation in these cases can exceed 15-fold (Rasenick et al., 1993; Popova et al., 1994).

Nucleotide cyclase activity in vertebrate photoreceptors, which use cyclic nucleotide–gated currents in sensory transduction, appears to be regulated 5–40-fold between light- and dark-adapted conditions, similar to the range of stimulation of AC observed here (Pace et al., 1985; Koutalos et al., 1995). Use of the protein per unit volume conversion factor allows comparison of the activities of AC in *Pleurobranchaea* and cyclase activity from vertebrate olfactory receptors and photoreceptors. Unstimulated levels of *Pleurobranchaea* AC were $5.86 \pm 2.12 \times 10^{-9}$ mol·min^{-1}·(mg protein)$^{-1}$. 5-HT-stimulated levels of AC were $39.18 \pm 7.62 \times 10^{-9}$ mol·min^{-1}·(mg protein)$^{-1}$. These ranges of cellular cAMP concentrations and cyclase activity are similar to vertebrate tissues that also express cyclic nucleotide–gated currents (Pace et al., 1985; Stryer, 1986; Breer et al., 1990; Koutalos et al., 1995).

Cyclic nucleotide–gated currents have been identified in a wide variety of tissues including vertebrate photoreceptors, vertebrate and invertebrate olfactory receptors, cochlear hair cells, cardiac myocytes, sperm cells, and cultured hippocampal neurons (Haynes and Yau, 1985; Fesenko et al., 1985; Nakamura and Gold, 1987; Firestein et al., 1991; Zufall et al., 1991; Kolesnikov et al., 1991; DiFrancesco and Tortora, 1991; Hatt and Ache, 1994; Weyand et al., 1994; Leinders-Zufall et al., 1995). Many other large, identified neurons of gastropod central nervous systems also express $I_{Na,cAMP}$ (Liberman et al., 1975; Green and Gillette, 1983; Aldenhoff et al., 1983; Kononenko et al., 1983; Connor and Hockberger, 1984, 1985; Gillette and Green, 1987; McCrohan and Gillette, 1988; Kehoe, 1990; Huang and Gillette, 1991, 1993; Price and Goldberg, 1993; Sudlow et al., 1993). For other cell types where cyclic nucle-

otide–gated ion current is prominent, the analytical approach introduced here with suitable modifications may complement conventional measures of cyclic nucleotides, particularly for the case of single cells that are too small to assay by presently available biochemical techniques. The general method may be adaptable by the use of caged cyclic nucleotides and several other possible indices of baseline current. Introduction of cyclic nucleotide–gated channels either genetically or directly to act as reporter ion channels may be practical in many types of cells. Aside from studies of neuromodulator-neurohormone actions as performed here, these methods are applicable to inquiries of receptor-G protein-AC coupling, interactions of other intracellular messenger pathways with cAMP metabolism, and the time course of cAMP fluctuations within which cAMP-dependent phosphorylation might be influenced.

APPENDIX

The derivation of the differential equation follows from that established for solutions in three dimensional electrotonus theory (Purves, 1976, 1977). The following normalized variables are used: $B = r_n(k_h/D)^{0.5}$, $R = r(k_h/D)^{0.5}$, where r, r_n, D, and k_h have the same meanings as in the text.

The general form of the differential equation describing movement of potential in a three-dimensional syncytium (Purves, 1976, 1977) as recast in terms of movement of ions. Since at steady state $dC/dt = 0$, the differential equation simplifies to:

$$C = \frac{1}{R}\frac{d^2RC}{dR^2} \tag{A1}$$

The general solution to Eq. A1 is:

$$RC = X_1e^{R} + X_2e^{-R} \tag{A2}$$

The following boundary conditions apply to Eq. A2:

$$\text{the initial conditions are: } 0 \le R \le B \tag{A3}$$

$$\text{impermeable cellular membrane at B: } R \le B \tag{A4}$$

source at radius R = B:

$$R^2\frac{dC}{dR} = \frac{Q}{4\pi D\sqrt{D/k_h}} \tag{A5}$$

Solving the subsidiary equations with the boundary conditions yields:

$$-X_2 = \frac{Q}{4\pi D\sqrt{D/k_h}}\frac{1}{B(e^{B} + e^{-B}) - (e^{B} - e^{-B})} \tag{A6}$$

The restriction $X_1 = -X_2$ must also be applied to Eq. A2 to prevent [cAMP] from approaching infinity as $R \rightarrow 0$ (Purves, 1976, 1977). Using the relationship from Eq. A6 and the restriction that $X_1 = -X_2$, Eq. A2 simplifies to Eq. 3.

We thank Mr. Robert Moats for assistance in performing the Bradford assays, Dr. Lia Faiman for her kind assistance with the biochemical measures, and Drs. Martha Gillette and Jonathan Sweedler for careful reading of the manuscript.

This work was supported by National Institutes of Health (RO1 NS26838) and National Science Foundation (IBN 88-21219).

Original version received 24 March 1997 and accepted version received 25 June 1997.

REFERENCES

Abrams, T.W., K.A. Karl, and E.R. Kandel. 1991. Biochemical studies of stimulus convergence during classical conditioning in *Aplysia*: dual regulation of adenylate cyclase by Ca^{2+}/calmodulin and transmitter. *J. Neurosci.* 11:2655–2665.

Aldenhoff, J.B., G. Hofmeier, H.D. Lux, and D. Swandulla. 1983. Stimulation of a sodium influx by cAMP in *Helix* neurons. *Brain Res.* 276:289–296.

Beavo, J.A., P.J. Bechtel, and E.G. Krebs. 1974. Activation of protein kinase by physiological concentrations of cyclic AMP. *Proc. Natl. Acad. Sci. USA.* 71:3580–3583.

Bacskai, B.J., B. Hochner, M. Mahaut-Smith, S.R. Adams, B.-K. Kaang, E.R. Kandel, and R.Y. Tsien. 1993. Spatially resolved dynamics of cAMP and protein kinase A subunits in *Aplysia* sensory neurons. *Science (Wash. DC).* 260:222–226.

Bolger, G.B. 1994. Molecular biology of the cyclic AMP-specific cyclic nucleotide phosphodiesterases: a diverse family of regulatory enzymes. *Cell. Signal.* 6:851–859.

Bradford, M.M. 1976. A rapid and sensitive method for the quantification of microgram quantities of protein utilizing the principle of protein-dye binding. *Anal. Biochem.* 72:248–254.

Breer, H., I. Boekhoff, and E. Tareilus. 1990. Rapid kinetics of second messenger formation in olfactory transduction. *Nature (Lond.).* 345:65–68.

Byrne, J.H., R. Zwartjes, R. Homayouni, S.D. Critz, and A. Eskin. 1993. Roles of second messenger pathways in neuronal plasticity and in learning and memory. *Adv. Second Messenger Phosphoprotein Res.* 27:47–108.

Connor, J.A., and P. Hockberger. 1984. A novel membrane sodium current induced by injection of cyclic nucleotides into gastropod neurones. *J. Physiol. (Cambr.).* 354:139–162.

Connor, J.A., and P. Hockberger. 1985. Calcium and cAMP: second messengers in gastropod neurons. *In* Model Neural Networks and Behavior. A.I. Selverston, editor. Plenum Press, New York. pp. 437–460.

DiFrancesco, D., and P. Tortora. 1991. Direct activation of cardiac pacemaker channels by intracellular cyclic AMP. *Nature (Lond.).* 351:145–147.

Eliot, L.S., Y. Dudai, E.R. Kandel, and T.W. Abrams. 1989. Ca^{2+}/calmodulin sensitivity may be common to all forms of neural adenylate cyclase. *Proc. Natl. Acad. Sci. USA.* 86:9564–9568.

Fell, D.A. 1980. Theoretical analyses of the functioning of the high and low-K_m cyclic nucleotide phosphodiesterase in the regulation of the concentration of adenosine 3′,5′-cyclic monophosphate in animal cells. *J. Theor. Biol.* 84:361–385.

Fesenko, E., S. Kolesnikov, and A. Lyubarsky. 1985. Induction by cyclic GMP of cationic conductances in plasma membrane of retinal rod outer segment. *Nature (Lond.).* 313:310–313.

Firestein, S., F. Zufall, and G.M. Shepherd. 1991. Single odor-sensitive channels in olfactory receptor neurons are also gated by cyclic nucleotides. *J. Neurosci.* 11:3565–3572.

Funte, L.R., and P.G. Haydon. 1993. Synaptic target contact enhances presynaptic calcium influx by activating cAMP-dependent protein kinase during synaptogenesis. *Neuron.* 10:1069–1078.

Gillette, M.U., and R. Gillette. 1983. Bursting neurons command consummatory feeding behavior and coordinated visceral receptivity in the predatory mollusk *Pleurobranchaea. J. Neurosci.* 3: 1791–1806.

Gillette, R., M.U. Gillette, and W.J. Davis. 1982. Substrates of command ability in a buccal neuron of *Pleurobranchaea. J. Comp. Physiol.* 146:461–470.

Gillette, R., and D.J. Green. 1987. Calcium dependence of voltage sensitivity in adenosine 3′:5′-cyclic phosphate-stimulated sodium current. *J. Physiol. (Cambr.)* 393:233–245.

Goldsmith, B.A., and T.W. Abrams. 1991. Reversal of synaptic depression by serotonin and *Aplysia* sensory neuron synapses involves activation of adenylyl cyclase. *Proc. Natl. Acad. Sci. USA.* 88:9021–9025.

Green, D.J., and R. Gillette. 1983. Patch- and voltage-clamp analysis of cyclic AMP-stimulated inward current underlying neurone bursting. *Nature (Lond.).* 306:784–785.

Greenberg, S.M., L. Bernier, and S.H. Schwartz. 1987. Distribution of cAMP and cAMP-dependent protein kinases in *Aplysia* Sensory neurons. *J. Neurosci.* 7:291–301.

Hatt, H., and B.W. Ache. 1994. Cyclic nucleotide- and inositol phosphate-gated ion channels in lobster olfactory receptor neurons. *Proc. Natl. Acad. Sci. USA.* 91:6264–6268.

Haynes, L., and K. Yau. 1985. Cyclic GMP-sensitive conductance in outer segment membrane of catfish cones. *Nature (Lond.).* 317: 61–64.

Hockberger, P., and T. Yamane. 1987. Compartmentalization of cyclic AMP elevation in neurons of *Aplysia californica. Cell. Mol. Neurobiol.* 7:19–33.

Hodgkin, A.L., and B.J. Nunn. 1988. Control of light-sensitive current in salamander rods. *J. Physiol. (Cambr.).* 403:439–471.

Huang, R.-C., and R. Gillette. 1991. Kinetic analysis of cAMP-activated Na^+ current in the molluscan neuron: a diffusion-reaction model. *J. Gen. Physiol.* 98:835–848.

Huang, R.-C., and R. Gillette. 1993. Coregulation of cyclic AMP-activated Na^+ current by Ca^{2+}. *J. Physiol. (Cambr.)* 462:307–320.

Kehoe, J. 1990. Cyclic AMP-induced slow inward current in depolarized neurons of *Aplysia californica. J. Neurosci.* 10:3194–3207.

Kirk, M.D., R. Taussig, and R.H. Scheller. 1988. Egg-laying hormone, serotonin, and cyclic nucleotide modulation of ionic currents in the identified motoneuron B16 of *Aplysia. J. Neurosci.* 8: 1181–1193.

Kolesnikov, S.S., T.I. Rebrik, A.V. Zhainazarov, G.A. Tavartkiladze, and G.R. Kalamkarov. 1991. A cyclic AMP-gated conductance in cochlear hair cells. *FEBS Lett.* 290:167–170.

Kononenko, N.I., P.G. Kostyuk, and A.D. Scherbatko. 1983. The effect of intracellular injections on stationary membrane conductances and voltage- and time-dependent ionic currents in identified snail neurons. *Brain Res.* 268:321–338.

Koutalos, Y., K. Nakatani, T. Tamua, and K.-W. Yau. 1995. Characterization of guanylate cyclase activity in single retinal rod outer segments. *J. Gen. Physiol.* 106:863–890.

Krnjević, K., J.F. Mitchell, and J.C. Szerb. 1963. Determination of iontophoretic release of acetylcholine from micropipettes. *J. Physiol. (Cambr.)* 165:421–436.

Leinders-Zufall, R., H. Rosenboom, C.J. Barnstable, G.M. Shepherd, and F. Zufall. 1995. A calcium-permeable cGMP-activated cation conductance in hippocampal neurons. *Neuroreport.* 6:45–49.

Liberman, E.A., S.V. Minina, and K.V. Golubtsov. 1975. The study of metabolic synapse: I. Effect of intracellular microinjection of 3′,5′ AMP. *Biophys. (Mosc.)* 20:451–457.

McCrohan, C.R., and R. Gillette. 1988. Cyclic AMP-stimulated sodium current in identified feeding neurons of *Lymnaea stagnalis. Brain Res.* 438:115–123.

Nakamura, T., and G. Gold. 1987. A cyclic nucleotide-gated conductance in olfactory receptor cilia. *Nature (Lond.).* 325:442–444.

Ocorr, K.A., E.T. Walters, and J.H. Byrne. 1985. Associative conditioning analog selectively increases cAMP levels of tail sensory neurons in *Aplysia. Proc. Natl. Acad. Sci. USA.* 82:2548–2552.

Pace, U., E. Hanski, Y. Salomon, and D. Lancet. 1985. Odorant-sensitive adenylate cyclase may mediate olfactory reception. *Nature (Lond.).* 316:255–258.

Popova, J.S., G.L. Johnson, and M.M. Rasenick. 1994. Chimeric $G_{\alpha s}/G_{\alpha i2}$ proteins define domains on $G_{\alpha s}$ that interact with tubulin for β-adrenergic activation of adenylyl cyclase. *J. Biol. Chem.* 269:21748–21754.

Price, C.J., and J.I. Goldberg. 1993. Serotonin activation of a cyclic AMP-dependent sodium current in an identified neuron from *Helisoma trivolvis. J. Neurosci.* 13:4979–4987.

Purves, R.D. 1976. Current flow and potential in a three-dimensional syncytium. *J. Theor. Biol.* 60:147–162.

Purves, R.D. 1977. The time course of cellular responses to iontophoretically applied drugs. *J. Theor. Biol.* 65:327–344.

Purves, R.D. 1981. Microelectrode Methods for Intracellular Recording and Ionophoresis. Biological Techniques Series. J.E. Treherne and P.H. Rubery, editors. Academic Press, London. 146 pp.

Rasenick, M.M., M. Lazarevic, M. Watanabe, and H.H. Hamm. 1993. Permeable cell systems as models for studying disruption, by site-specific synthetic peptides, of receptor-G protein-effector coupling. *Methods Enzymol.* 5:252–257.

Shakur, Y., J.G. Pryde, and M.D. Houslay. 1993. Engineered deletion of the unique N-terminal domain of the cyclic AMP-specific phosphodiesterase RD1 prevents plasma membrane association and the attainment of enhanced thermostability without altering its sensitivity to inhibition by rolipram. *Biochem. J.* 292:677–686.

Siegelbaum, S.T., J.S. Camardo, and E.R. Kandel. 1982. Serotonin and cyclic AMP close single K^+ channels in *Aplysia* sensory neurons. *Nature (Lond.).* 299:413–417.

Stryer, L. 1986. Cyclic GMP cascade of vision. *Annu. Rev. Neurosci.* 9: 87–119.

Sudlow, L.C., R.-C. Huang, D.J. Green, and R. Gillette. 1993. cAMP-activated Na^+ current of molluscan neurons is resistant to kinase inhibitors and is gated by cAMP in the isolated patch. *J. Neurosci.* 13:5188–5193.

Sudlow, L.C., and R. Gillette. 1995. Cyclic AMP-gated sodium current in neurons of the pedal ganglion of *Pleurobranchaea californica* is activated by serotonin. *J. Neurophysiol. (Bethesda).* 73:2230–2236.

Walsh, J.P., and J.H. Byrne. 1989. Modulation of a steady-state Ca^{2+}-activated, K^+ current in tail sensory neurons of *Aplysia*: role of serotonin and cAMP. *J. Neurophysiol. (Bethesda).* 61:32–44.

Weyand, I., M. Godde, S. Frings, J. Weiner, F. Muller, W. Altenhofen, H. Hatt, and U.B. Kaupp. 1994. Cloning and functional expression of a cyclic-nucleotide-gated channel from a mammalian sperm. *Nature (Lond.).* 368:859–863.

Wilson, G.F., and L.K. Kaczmarek. 1993. Mode-switching of a volt-

age-gated cation channel is mediated by a protein kinase A-regulated tyrosine phosphatase. *Nature (Lond.)*. 366:433–438.

Yovell, Y., and T.W. Abrams. 1992. Temporal asymmetry in activation of *Aplysia* adenylyl cyclase by calcium and transmitter may explain temporal requirements of conditioning. *Proc. Natl. Acad. Sci. USA*. 89:6526–6530.

Yovell, Y., E.R. Kandel, Y. Dudai, and T.W. Abrams. 1987. Biochemical correlates of short-term sensitization in *Aplysia*: temporal analysis of adenylate cyclase stimulation in a perfused-membrane preparation. *Proc. Natl. Acad. Sci. USA*. 84:9285–9289.

Zufall, F., S. Firestein, and G.M. Shepherd. 1991. Analysis of single cyclic nucleotide-gated channels in olfactory receptor cells. *J. Neurosci*. 11:3573–3580.